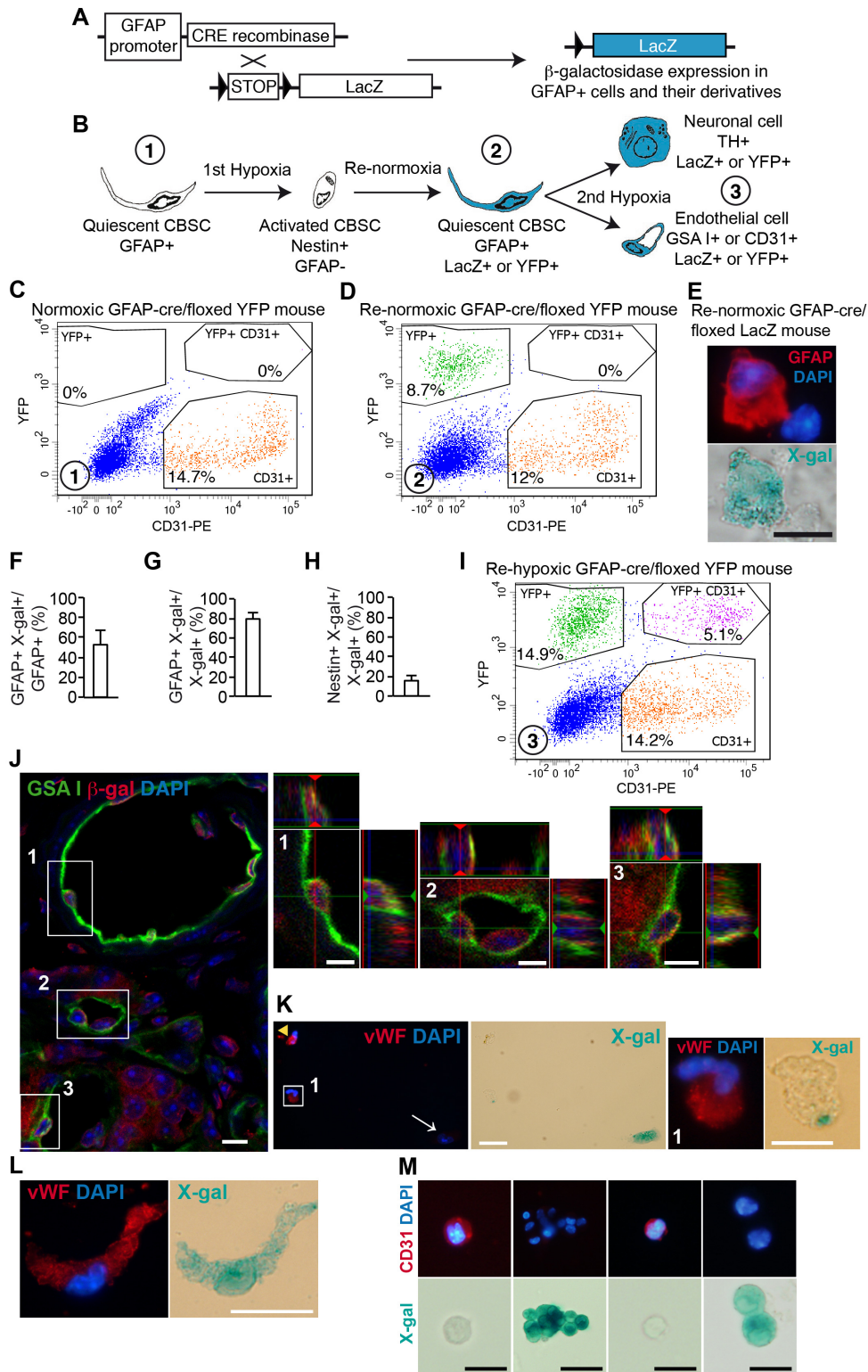


**Cell Reports, Volume 19**

**Supplemental Information**

**Physiological Plasticity of Neural-Crest-Derived  
Stem Cells in the Adult Mammalian Carotid Body**

**Valentina Annese, Elena Navarro-Guerrero, Ismael Rodríguez-Prieto, and Ricardo Pardal**



**Figure S1. Cell fate mapping in the adult carotid body stem cell niche, Related to Figure 1.**

(A) Diagram illustrating the CRE recombinase-mediated recombination event taking place in GFAP+ cells of *GFAP-Cre/floxed LacZ* mice to allow the expression of the reporter gene. Note that this recombination is irreversible, producing the labeling of all GFAP+ cell derivatives and hence enabling the cell fate mapping.

(B) Scheme of the cellular events taking place in the CB of *GFAP-Cre/floxed LacZ* or *YFP* mice during the first two expositions to hypoxia. The human origin of the GFAP promoter used in these transgenic animals makes the construct to behave as an inducible Cre, with the first exposure to hypoxia functioning

as the trigger stimulus to the expression of the recombinase.

(C) FACS plot showing CD31<sup>+</sup> endothelial cells and YFP<sup>+</sup> cells within the CB of *GFAP-Cre/floxed YFP* mice before the first exposure to hypoxia. Note the complete absence of recombined YFP<sup>+</sup> cells.

(D) FACS plot showing CD31<sup>+</sup> endothelial cells and YFP<sup>+</sup> cells within the CB of a re-normoxic *GFAP-Cre/floxed YFP* mouse after the first exposure to hypoxia. Note the presence of YFP<sup>+</sup> cells but without conversion into endothelial cells yet (absence of double positive cells).

(E) Fluorescent and bright field pictures of two CB dispersed cells from a re-normoxic *GFAP-Cre/floxed LacZ* mouse, illustrating the specific expression of the reporter enzyme in the GFAP<sup>+</sup> cell. Scale: 10  $\mu\text{m}$ .

(F) Quantification of GFAP/X-gal double positive cells among GFAP<sup>+</sup> cells from dispersed CB of re-normoxic *GFAP-Cre/floxed LacZ* mice, illustrating that about half of GFAP<sup>+</sup> cells get labeled after the first exposure to hypoxia. n=3 CB enzymatic cell dispersions (2 mice each cell dispersion).

(G, H) Quantification of GFAP<sup>+</sup> (G) and Nestin<sup>+</sup> (H) cells within X-gal<sup>+</sup> cells in dispersed CB of re-normoxic *GFAP-Cre/floxed LacZ* mice, indicating that all labeled cells are GFAP<sup>+</sup> stem cells with some basal activation of these cells to Nestin<sup>+</sup> progenitors. n=3 CB enzymatic cell dispersions (2 mice each cell dispersion). No single CD31/X-gal double positive cell was found in these preparations, consistent with the results obtained by FACS (D).

(I) FACS plot showing YFP signal and CD31 staining in dispersed CB cells from *GFAP-Cre/floxed YFP* mouse after the second exposure to hypoxia. In this case, the presence of CD31/YFP double positive cells indicate that some labeled GFAP<sup>+</sup> stem cells have undergone differentiation into endothelial cells.

(J) Confocal image of  $\beta$ -galactosidase (red) and GSA I (green) immunofluorescence performed on CB sections from *GFAP-Cre/floxed LacZ* mice. A higher magnification of the boxed regions depicted in (J), showing Z-axis projection views, is shown in (J1), (J2) and (J3). Scale bars: 5  $\mu\text{m}$ .

(K, L) Examples of vWF<sup>+</sup> endothelial cells derived from CBSCs (vWF<sup>+</sup> X-gal<sup>+</sup>) and detected in dispersed CBs from hypoxic *GFAP-Cre/floxed LacZ* mice. (K1) Zoom of the boxed area in (K). Note in (K) the presence of a vWF<sup>+</sup> endothelial cell not derived from CBSCs (yellow arrow head) and an unidentified X-gal<sup>+</sup> cell (white arrow). Scale bars: 5  $\mu\text{m}$ .

(M) Pictures showing the combination of CD31 immunolabeling with X-gal staining in dispersed CB cells from *TH-Cre/floxed LacZ* mice. No double positive cells were observed in any mice. n=3 CB enzymatic cell dispersions (2 mice each cell dispersion). Scale bars: 20  $\mu\text{m}$  in the second column and 10  $\mu\text{m}$  in the rest of columns.

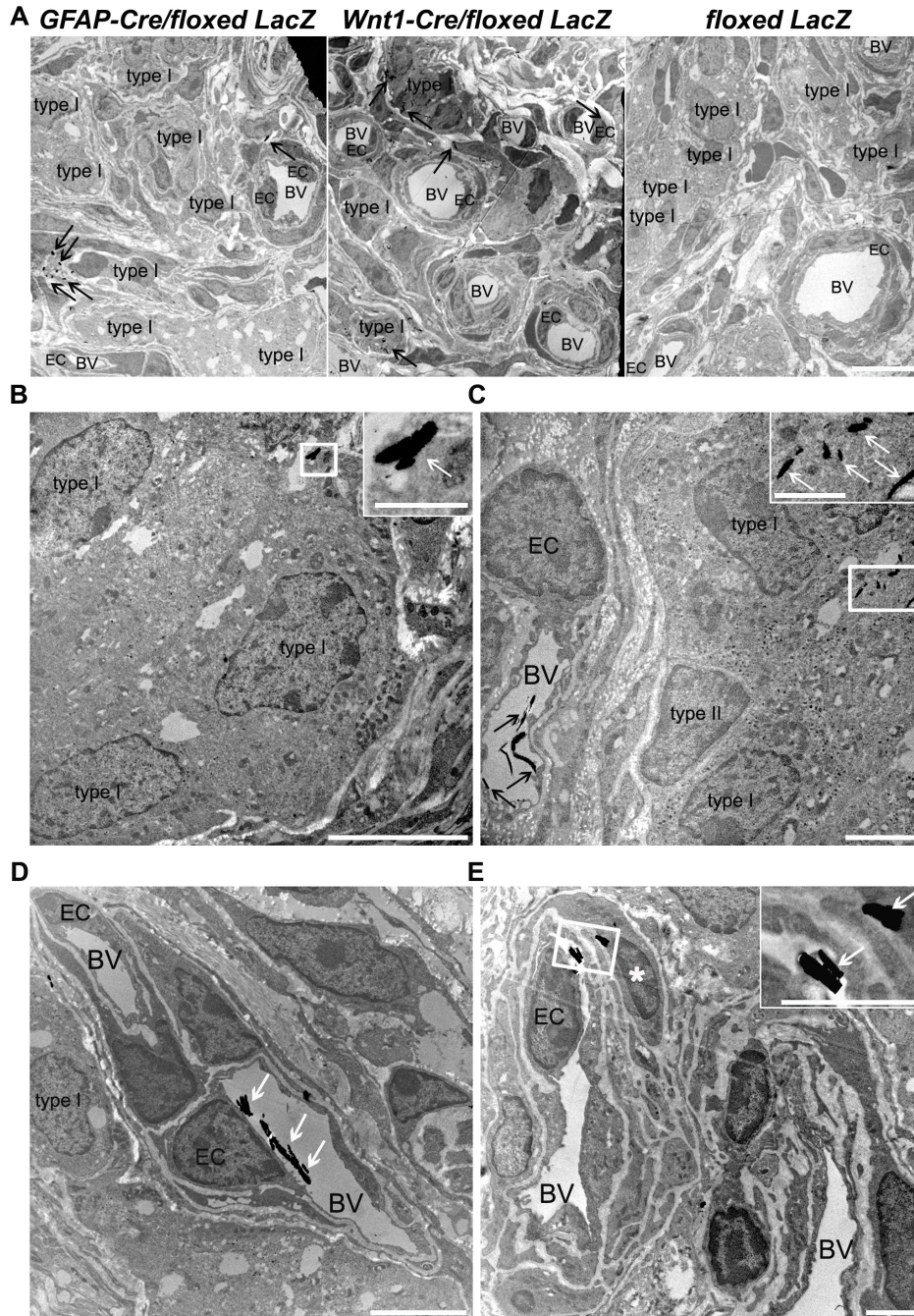


**Figure S2. Electron microscopy corroborates GFAP+ progenitors giving rise to type I and endothelial cells in response to hypoxia, Related to Figure 1.**

Bluo-gal is an alternative substrate for the  $\beta$ -gal enzyme, similar to X-gal, but the resulting electron dense precipitate is detectable by EM (Weis et al., 1991; Joseph et al., 2004).

(A) Low magnification electron micrographs of CB sections from *GFAP-cre/floxed LacZ*, *Wnt1-cre/floxed LacZ*, and control *floxed LacZ* mice. Dark arrows indicate Bluo-gal crystals in both *Wnt1-cre* and *GFAP-cre/floxed LacZ* strains. The level of bluo-gal staining in the CB of *GFAP-cre/floxed LacZ* mice was much lower than in the *Wnt1-cre/floxed LacZ* mice, consistent to what has been shown before for X-gal staining (Pardal et al., 2007). Note the total absence of Bluo-gal staining in the control *floxed LacZ* littermate mouse. Scale bar: 10  $\mu$ m.

(B-E) Electronic micrographs of the CB of a *GFAP-Cre/floxed LacZ* mouse dissected and processed for Bluo-gal staining. Upon  $\beta$ -galactosidase action, Bluo-gal forms an electron-dense precipitate, visible as small black crystals (arrows) by electron microscopy. In addition to neuronal type I cells (B and C), recognized by the presence of dense-core vesicles, abundant mitochondria, and the typical condensation

of chromatin, we observed ECs, structurally identified at the wall of blood vessels, labeled with bluogal precipitates, which typically appeared in the vessel lumen (C-E). In some of these vessels, labeled cells with the typical shape of smooth muscle, surrounding the endothelium, could be observed (asterisk in (E)). No single bluogal positive cell was found in *flxed LacZ* control mice (A). Cellular plasma membrane appears light and fragmented due to the required fixation conditions, which provokes the diffusion of Bluogal precipitates out of the cells. Scale bars: 5  $\mu\text{m}$  in (B) and (D); 2  $\mu\text{m}$  in (C), (E) and inset in (E); 1  $\mu\text{m}$  in insets in (B) and (C). n=3 animals.

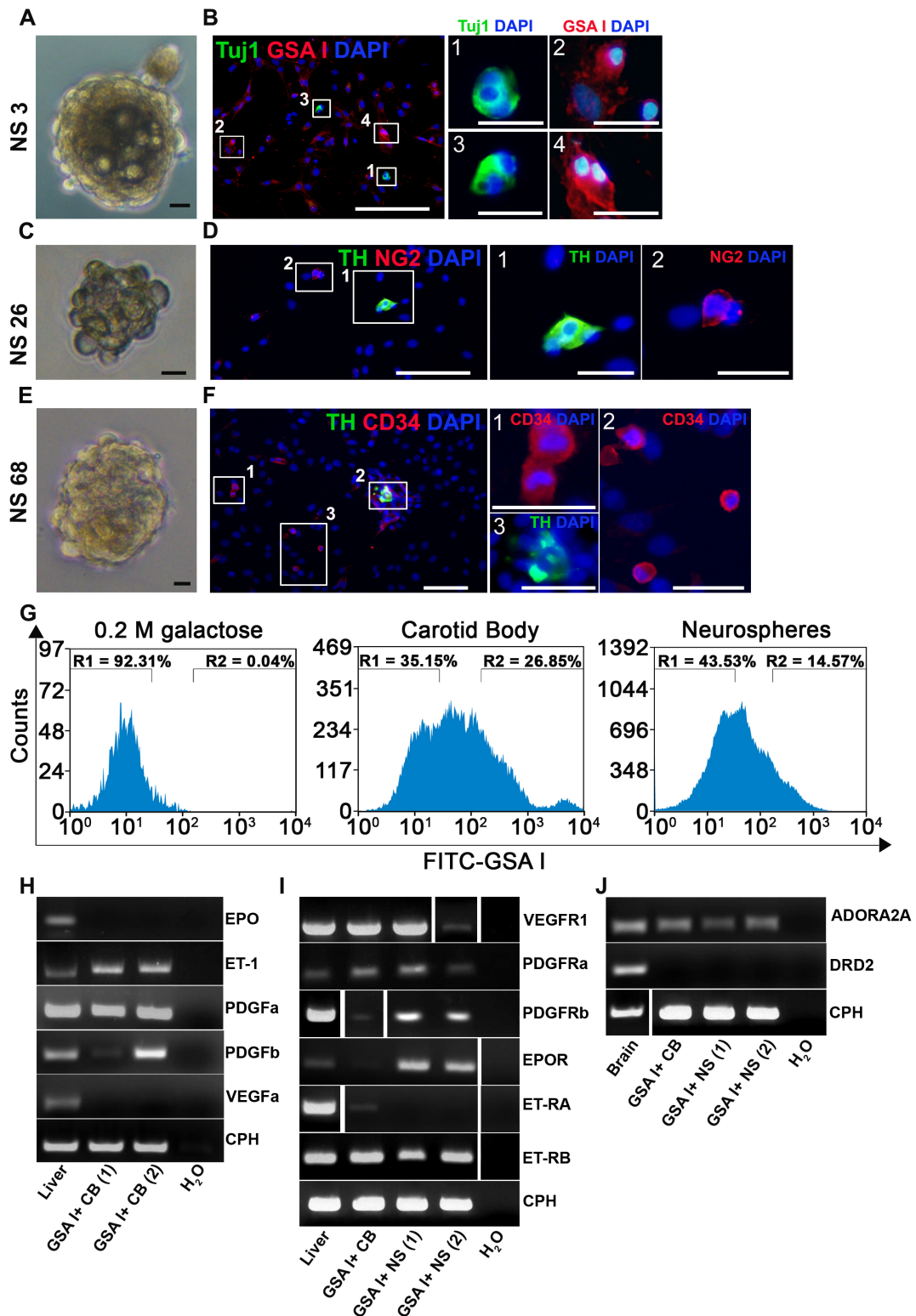


**Figure S3. Single NS progenitor cells display multipotency *in vitro*, and CB GSA I+ endothelial cells are a source of vascular factors, Related to Figures 2 and 3.**

(A, C, E) Bright field photographs of secondary neurospheres formed after 2 weeks in culture from single progenitors derived from enzymatic dispersion of primary neurospheres. Scale bars: 5  $\mu$ m.

(B, D, F) Pictures showing the generation of both neuronal and mesodermal cells within the colonies obtained from single neurosphere-derived progenitor cells (NSPC). Co-existence of different cellular markers was proved inside the same colony (Tuj1 (green) and GSA I (red) in (B), TH (green) and NG2 (red) in (D), and TH (green) and CD34 (red) in (F)). Scale bars: 100  $\mu$ m. On the most right panels, high

magnification images of the areas boxed in (B), (D) and (F), are shown. Scale bars: 10  $\mu\text{m}$  in (B1-4); 30  $\mu\text{m}$  in (D1-2) and in (F1-2); and 50  $\mu\text{m}$  in (F3). n=4 primary NS cultures.

(G) Analysis by flow cytometry of both rat CB and adherent neurosphere cells using GSA I lectin as an endothelial marker. A negative control using galactose is shown in the left panel.

(H) RT-PCR analysis in sorted GSA I<sup>+</sup> cells (R2) from two different CBs, showing expression of vascular factors. Rat liver was used as positive control, and cyclophilin (CPH) was used as a loading control.

(I) RT-PCRs revealing expression of vascular factor receptors in rat liver and in GSA I<sup>+</sup> cells isolated from CB or adherent neurospheres by flow cytometry. Loading control used was cyclophilin (CPH).

(J) RT-PCR displaying presence of ADORA2A mRNA in GSA I<sup>+</sup> cells sorted from CB or adherent neurospheres by flow cytometry. DRD2 mRNA resulted below detection levels by RT-PCR (40 cycles) in GSA I<sup>+</sup> cells obtained from both CB and neurospheres. Rat brain was used as positive control. Loading control was CPH. RNA expression for each gene was studied using 3 different RNA extractions obtained by cell sorter separation from 3 independent CB dispersions.

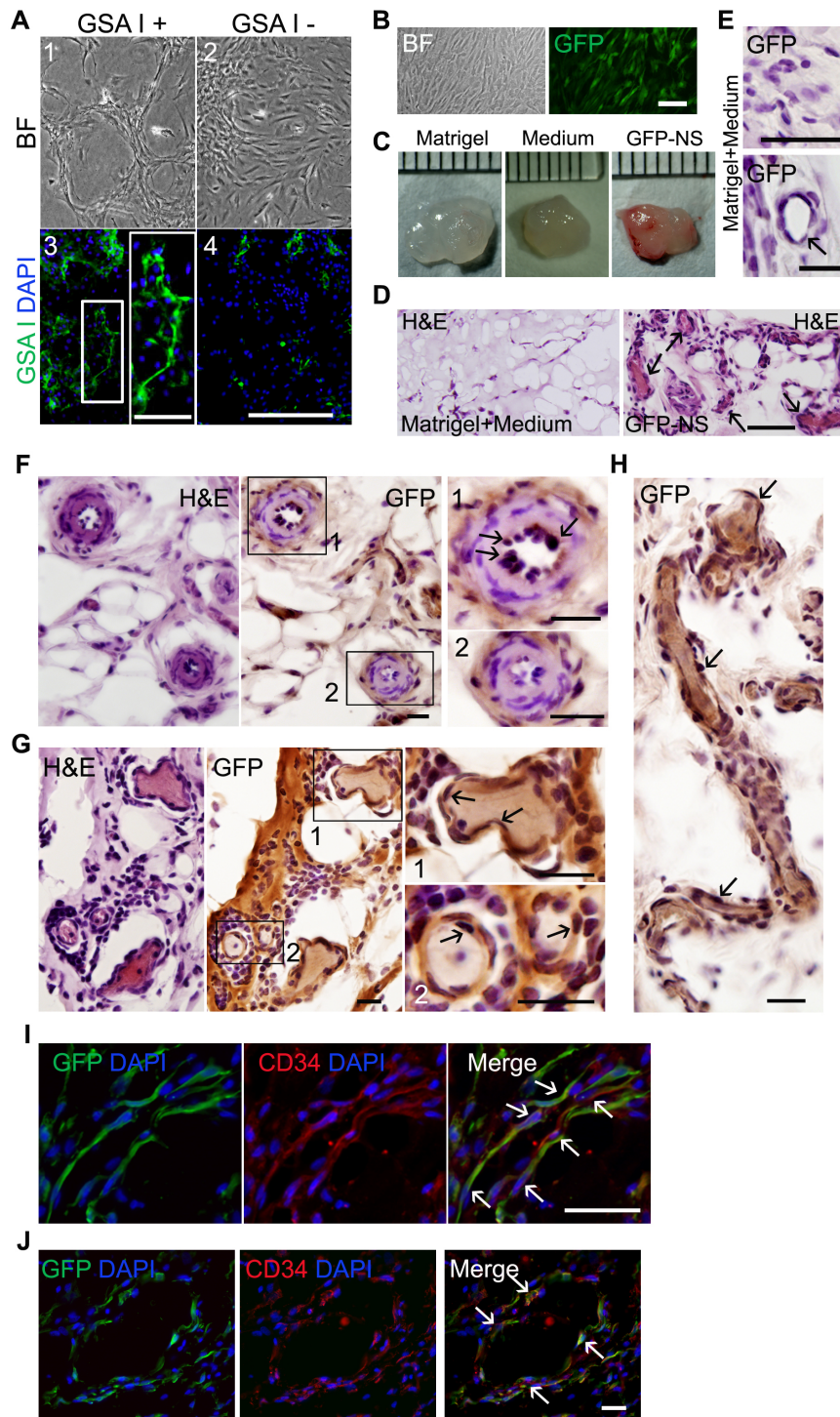


**Figure S4. Vasculogenic potential of CBSC-derived NS cells, Related to Figure 3.**

In order to test the vasculogenic potential of CB progenitor cells, we used NS cells, instead of FACS isolated CBSCs, due to the need for high cell numbers in these assays.

(A) Analysis by both phase contrast (1-2) and fluorescence (3-4) microscopy of the viability of an angiogenesis assay performed on matrigel coated plates (Benelli and Albini, 1999). Note how GSA I+ cells exhibit higher level of structural organization and a tendency to form multiple links between cells (1, 3) when compared to the GSA I negative cell fraction (2, 4). Scale bars: 500  $\mu\text{m}$ , and 100  $\mu\text{m}$  in the inset. n=3 independent experiments.

(B) Phase contrast (left panel) and fluorescence (right panel) representative photographs of NS cells infected with VSV-G pseudotyped lentiviral vector particles. Efficiency of infection was measured by GFP expression using fluorescence microscopy. Scale bar: 100  $\mu\text{m}$ . n=3.



(C) Macroscopic view of matrigel plugs from an *in vivo* vasculogenesis assay, in which NS cells labeled with GFP (GFP-NS; panel B) were suspended in matrigel and injected subcutaneously in recipient animals (Melero-Martin et al., 2007), which are then exposed to hypoxia for one week. From left to right: matrigel plugs containing PBS alone, medium alone, and GFP-NS cells, harvested one week after implantation. Upon dissection of the transplants, reddish areas could be observed in NS cell-containing matrigels, but not in matrigel only or matrigel plus medium control transplants. Rulers are in mm.

(D) Hematoxylin/eosin (H&E) staining of implant thin sections containing medium alone (left) or GFP-NS cells (right). Note the presence of microvessels in the implant containing GFP-NS cells (arrows in the right panel), which were absent in control transplants. Scale bar: 100  $\mu$ m.

(E) Bright field pictures of frozen sections of medium-containing matrigel plugs (negative control), subjected to immunostaining for GFP reporter protein. No GFP<sup>+</sup> cells were detected, demonstrating the specificity of the antibody reaction. Few (arrow in the lower panel) or no vascular structures were observed in sections obtained from this type of negative control matrigel plugs. Scale bars: 50  $\mu$ m in upper panel and 20  $\mu$ m in lower panel.

(F, G) H&E and immunohistochemical staining with specific anti-GFP antibody of adjacent serial sections of matrigel plug containing GFP-NS cells one week after implantation, revealing that GFP-expressing NS cells contributed to the endothelial wall of blood-containing vessels (arrows in panels F1, G1, and G2). No GFP positive cells were found in sections from plugs with only medium (panel E). Some vessels completely negative for the GFP marker were also observed (panel F2), likely due to contribution of host-derived mesenchymal cells.

(H) Detail of a long vessel with numerous GFP immuno-positive cells in the wall (see arrows), confirming donor contribution to the assembled microvessels. Scale bars in (F), (G), and (H): 20  $\mu$ m. n=3 transplanted rats.

(I, J) Fluorescent pictures showing blood vessels in NS cell-containing matrigel plugs, after 7 days of exposition to hypoxia. Detection of CD34 (red) and GFP (green) double positive endothelial cells (see arrows in merged pictures) confirmed NS cell-derived contribution to new vessel formation in matrigel plugs. Scale bars: 100  $\mu$ m in (I) and 20  $\mu$ m in (J).

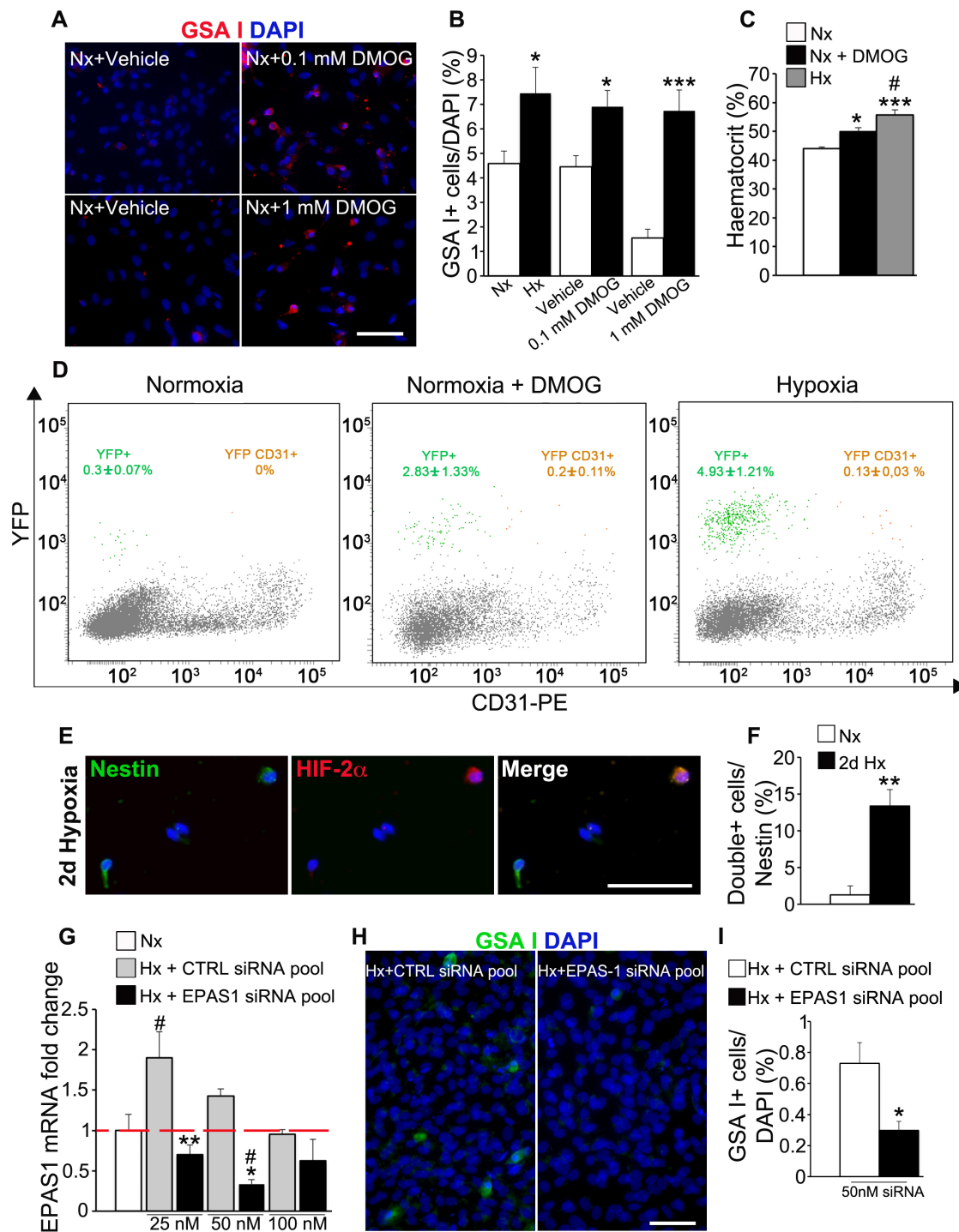


**Figure S5. HIF-2 $\alpha$  contributes to CBSC activation and endothelial differentiation, Related to Figure 4.**

Inhibition of PHDs by lack of oxygen allows stabilization of HIFs, which in turn control the expression of a wide variety of hypoxia-sensitive genes (Kaelin and Ratcliffe, 2008).

(A) Immunofluorescent micrographs illustrating endothelial differentiation (GSA I+ cells in red) from NS cells cultured in adherent conditions on fibronectin, and in the presence of vehicle (left panel) or DMOG (right panel) in normoxic environment (Nx). Scale bar: 50  $\mu$ m. Dimethylxalylglycine (DMOG), elicited a similar increase in endothelial differentiation to that obtained by low oxygen (Figure 3A and B).

(B) Bar graph summarizing the percentage of GSA I+ cells (n=4 independent cultures) in adherent NS cells cultured under normoxia (Nx) or hypoxia (Hx), under normoxia in the presence of vehicle or 0.1 mM

DMOG, and under normoxia in the presence of vehicle or 1 mM DMOG. Data are represented as mean±s.e.m. \* $p \leq 0.05$ , \*\*\* $p \leq 0.001$ , Student's t test comparing each treatment group (Hx, 0.1 mM DMOG, and 1 mM DMOG) to their respective control (Nx, and vehicles).

(C) Quantification of haematocrit in *GFAP-Cre/floxed YFP* mice exposed to hypoxia (10% O<sub>2</sub>, grey bar) or maintained in normoxic conditions and treated with DMOG (black bar), in comparison to normoxic untreated mice (white bar). Data is represented as mean±s.e.m.; One-Way ANOVA Tukey's multiple comparisons post hoc test compared to normoxia, \* $p \leq 0.05$ , \*\*\* $p \leq 0.001$ , or compared to hypoxia, # $p \leq 0.05$  (n=6-7 mice). A clear but discrete increase in haematocrit was observed in DMOG-infused animals when compared to hypoxic animals.

(D) Cell fate mapping study performed by FACS analysis in dissociated CB cells from normoxic, normoxic plus injected DMOG (12 days), and hypoxic (12 days), *GFAP-Cre/floxed YFP* mice. Mean percentage values with standard errors for both YFP+ (green dots) and YFP+/CD31+ (orange dots) populations are reported in the plots. FACS plots are representative for 3 independent CB dispersions for each experimental group. Note how DMOG induced a clear increase in the number of YFP+ cells, including endothelial differentiation (CD31+), when compared to normoxic conditions, although the effect was more discrete than the one produced by hypoxia.

(E) Fluorescence micrographs illustrating stabilization of HIF-2 $\alpha$  in activated progenitor cells (nestin+ and round) in hypoxic conditions. Rat CBSCs usually display cellular prolongations when they are quiescent, and become round and proliferative when activated (Pardal et al., 2007). The pictures show an example of a CBSC still with a cell prolongation, negative for HIF, and an activated round nestin+ CBSC, which clearly underwent HIF stabilization. Scale bar: 50  $\mu$ m.

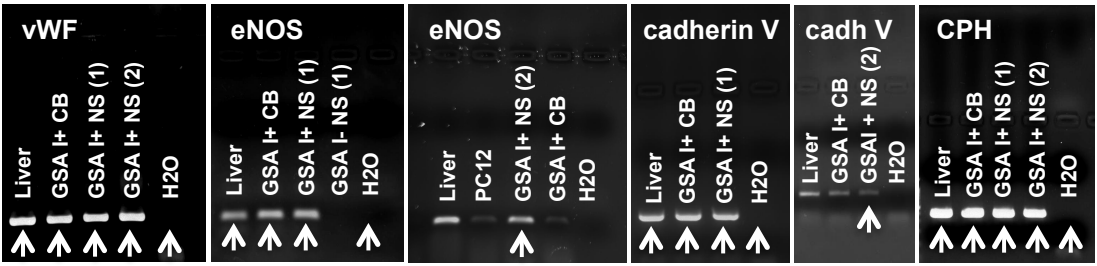
(F) Bar graph indicating the percentage of HIF-2 $\alpha$ + cells within nestin+ cell population, in both normoxic (white bar) and 2 days hypoxic CBs (black bar). The proportion of nestin+ progenitors that stabilize HIF, dramatically increases after only 2 days in hypoxic conditions (n=3 independent CB dispersions from 2 rats each). Data is represented as mean±s.e.m.; \*\* $p \leq 0.01$ , Student's t test compared to normoxic group.

(G) Specific inhibition of EPAS1 (the gene encoding for HIF2 $\alpha$ ) mRNA expression in dissociated NS cells transfected with different concentrations of EPAS1 siRNA pool (n=4 independent NS cultures). Data is represented as mean±s.e.m.; One-Way ANOVA Newman-Keuls multiple comparisons post hoc test compared to respective control (CTRL) pool concentration, \* $p \leq 0.05$ , \*\* $p \leq 0.01$ , or compared to normoxic conditions, # $p \leq 0.05$ . Transfection with EPAS1 siRNA not only prevented hypoxia-induced increase in EPAS1 expression but also decreased EPAS1 basal expression when compared to normoxic conditions.

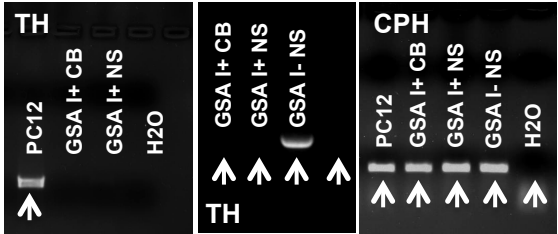
(H) Representative immunofluorescence pictures showing endothelial differentiation in enzymatically dispersed NS cells transfected with control siRNA pool (left panel) or EPAS1 siRNA pool, both under hypoxic conditions. Scale bar: 50  $\mu$ m.

(I) Quantification of the percentage of GSA I+ cells differentiated from both CTRL-interfered (white bar) or EPAS1-interfered (black bar) NS cells in hypoxic conditions (n=3 independent NS cultures). Data is represented as mean±s.e.m.; \* $p \leq 0.05$ , Student's t test compared to Hx+CTRL siRNA pool group. Knocking-down HIF2 $\alpha$  in NS progenitor cells clearly decreases the ability of these cells to convert into endothelial cells, clearly confirming an important role for PHD/HIF pathway in endothelial differentiation from CBSCs. These data demonstrate that CBSC differentiation into endothelial cells is directly sensitive to hypoxia, with a clear role of PHD/HIF system in the process. Therefore, hypoxia directly favors differentiation from CBSCs into both neuronal (Platero-Luengo et al., 2014) and endothelial lineages, being cell fate choice apparently more dependent on the presence of paracrine signaling. HIF factors include a number of different isoforms. HIF1 $\alpha$  has been involved in neural crest proliferation and specification (Barriga et al., 2013), although it does not seem to play a role in CB growth (Platero-Luengo et al., 2014; Hodson et al., 2016). In contrast, HIF2  $\alpha$  has been recently described to have an important role in hypoxia acclimatization (Arsenault et al., 2013; Bishop et al., 2013), and more specifically in CB growth (Hodson et al., 2016). Our data confirm HIF2 $\alpha$  as an important player in the induction of angiogenesis from CBSCs.

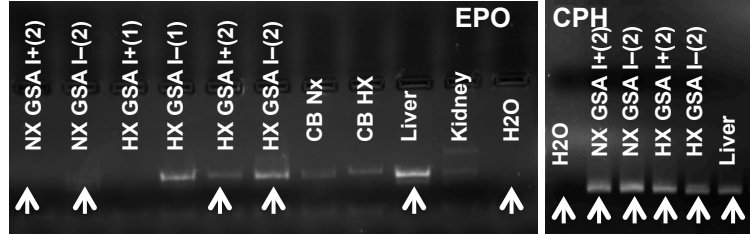
Related to Figure 3E



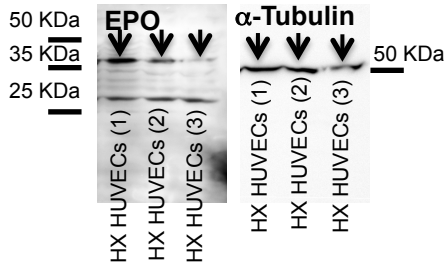
Related to Figure 3F



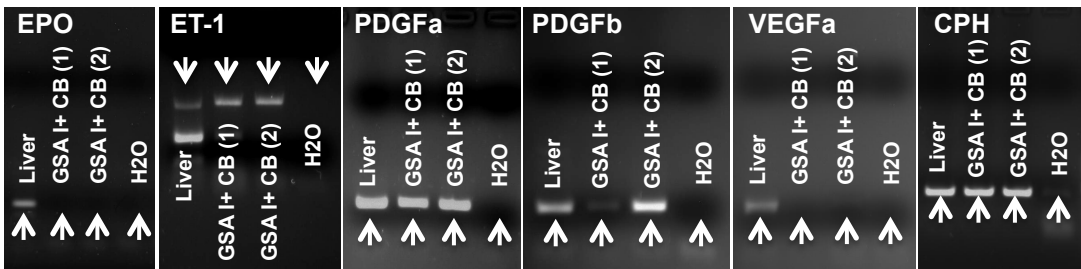
Related to Figure 4F



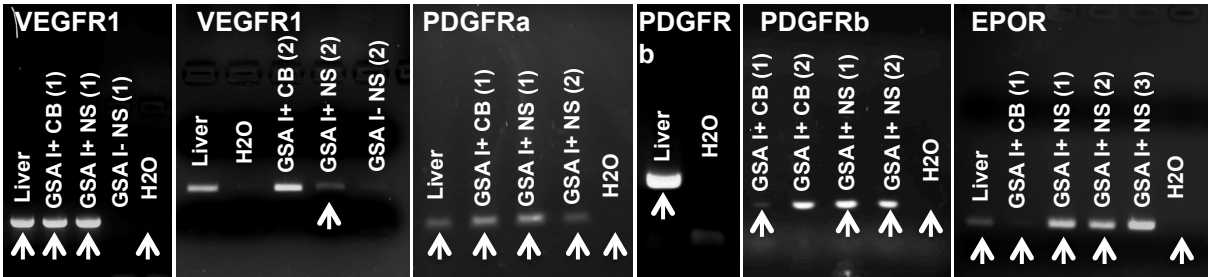
Related to Figure 4H



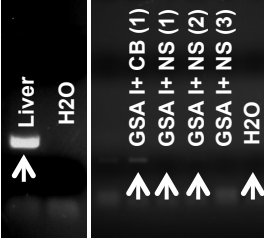
Related to Figure S3H



Related to Figure S3I



ET-RA



ET-RB

CPH



Related to Figure S3J

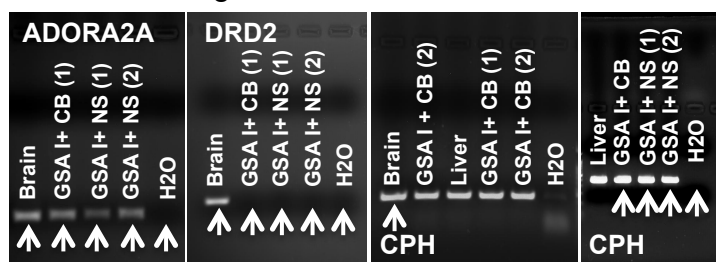


Figure S6. Original gels for PCRs and Western Blot, Related to Figures 3, 4, and S3.

Arrows point to the lanes used at the referred figures. All experiments and samples were run at the same time.

**Table S1. Antibodies and reagents, Related to Experimental Procedures.**

<b>Name</b>	<b>Concentration</b>	<b>Use</b>
Rb anti-TH, Novus Biological	1:1000	IHC, ICC
Chicken anti- $\beta$ -galactosidase, Novus Biological	1:200	IHC
Rb anti-Tuj1, Abcam	1:500	ICC
Ms anti-smooth muscle actin (SMA), Sigma	1:500	ICC
Rb anti GFP, Invitrogen	1:500	ICC, IHC
Rb anti-GFAP, Dako	1:500	ICC
Ms anti-Nestin, Merck Millipore	1:500	ICC
Rb anti-GFP and YFP, Invitrogen	1:500	IHC
Ms anti-NG2 proteoglycan	1:500	ICC
Rb anti-Von Willebrand Factor, Sigma	1:200	ICC
Gt anti CD34, R&D	1:100	ICC, IHC
Gt anti-EPO, Santa Cruz	1:200	WB
PE-Rat anti-mouse CD31, BD	1:100	FC, ICC
Rb anti HIF-2a, Novus Biological	1:100	ICC
Alexa488-donkey-anti-rabbit IgG, Molecular Probes	1:1000	IHC, ICC
Alexa488-donkey-anti-mouse-IgG, Molecular Probes	1:1000	IHC, ICC
Alexa568-donkey-anti-Chicken IgG, Molecular Probes	1:1000	IHC, ICC
Alexa488-donkey-anti-Chicken, Molecular Probes	1:1000	ICC
Alexa568-donkey-anti-Goat IgG, Molecular Probes	1:1000	ICC
Rhodamine-Griffonia Simplicifolia lectin I, Vector Labs	1:100	IHC, ICC
FITC-Griffonia Simplicifolia lectin I, Vector Labs	1:100	IHC, ICC
5-bromo-3-indolyl- $\beta$ -D-galactoside (bluo-gal), Invitrogen Life Technologies	2mM	EM
X-gal, Molecular Probes	2mM	ICC
DiI-labeled acetylated low density lipoproteins (DiI-AcLDL), Molecular Probes, Invitrogen	10 $\mu$ g/ml	ICC
7-AAD, Molecular Probes	2 mg/ml	FC

IHC= Immunohistochemistry; ICC= Immunocytochemistry; EM= Electron Microscopy; FC= Flow Cytometry

**Table S2. Sequences of oligonucleotides used as primers, Related to Experimental Procedures.**

<b>mRNA</b>	<b>sense</b>	<b>Sequence (5'→3')</b>	<b>Reference/Software</b>
vWF	F R	CACTGCCCTCCAGGGAAAAT CGGATGCGCTTCTGAGAGAT	Primer Blast (NCBI)
eNOS	F R	GGATCCAGTGGGGGAAACTG TGGCTGAACGAAGATTGCCT	Primer Blast (NCBI)
VEGFa	F R	TTTTCGTCCAACCTTCTGGGC TTCACCACTTCATGGGCTTTCT	Primer Blast (NCBI)
VEGFR1	F R	TTCCGGACTTTCAACACCTC CACCGAATAGCGAGCAGATT	Primer Blast (NCBI)
PDGFa	F R	GGAGCCATTCCCGCAGTTTG TCACCTCACATCCGTCTCCT	Primer Blast (NCBI)
PDGFb	F R	GCACCAATGCCAACTTCCTG GTTTGAGGTGTCTTGGCTCG	Primer Blast (NCBI)
PDGFRa	F R	TTCGCCAAGGTGGAAGAGAC ATCCCAAGATCCGACCAAGC	Primer Blast (NCBI)
PDGFRb	F R	GCGAAAACCTGTCACCCACAC AGAGTGCCTCCAGAACAAG	Primer Blast (NCBI)
EPO	F R	TACGTAGCCTCACTTCACTGCT CAGGTCACCTGTCCCCTCTC	Primer Blast (NCBI)
EPOR	F R	CGTCGAGTTTTGTGCCACTG GTCCAAGTCGCTAGCAGTCA	Primer Blast (NCBI)
ADORA2A	F R	GGCCGTGTGGATCAACAGTA AAGCCATTGTACCGGAGTGG	Primer Blast (NCBI)
DRD2	F R	CCAGTGAACAGGCGGAGAAT GTTTTGCCATTGGGCATGGT	Primer Blast (NCBI)
Enkephaline	F R	TACCTGCGCCATCTGAACAA TCTTGGCTAGCAAGTGGCTC	Primer Blast (NCBI)
ET-1	F R	ATCATCTGGGTCAACACTC GAATCTCCTGGCTCTCTG	(Kugelmeier et al., 2008)
ET <sub>A</sub>	F R	TTCGTCATGGTACCCTTCGA GATACTCGTTCATTTCATGG	(Kugelmeier et al., 2008)
ET <sub>B</sub>	F R	TTCACCTCAGCAGGATTCTG AGGTGTGGAAAGTTAGAACG	(Kugelmeier et al., 2008)
Cdh5	F R	GCACAGGCGGGTGTGAGCAT TCTCTCTGGGCCCTCCGTGC	Primer Blast (NCBI)
TH	F R	GGACATTGGACTTGCATCTCTGGG TGAGAAGCAGTGTGGGAGGATGG	Primer Express
EPAS1 Q	F R	GCAGATGGATAACTTGTACCTGAAAG CTGACAGAAGATCATATCACCGTCTT	Primer Blast (NCBI)
GLUT1 Q	F R	CCCGCTTCTCTGCTCATCAA GACCTTCTTCTCCCGCATCA	Primer Blast (NCBI)
VEGFa Q	F R	CGCAAGAAATCCCGGTTTAA CAAATGCTTTCTCCGCTCTGA	Primer Blast (NCBI)

F, forward; R, reverse; Q, control.

## Supplemental Experimental Procedures

### ***In Vivo* Hypoxic Treatments and Drug administration**

Transgenic mice (4-6 weeks old or 8-9 months old for DMOG *in vivo* experiments) and rats (6 weeks old) were chronically exposed to a 10% O<sub>2</sub> environment during 7 days by using a specially designed hermetic isobaric chamber, with O<sub>2</sub> and CO<sub>2</sub> controls, and temperature and humidity monitoring (Coy Laboratory Products, Inc.; Grass Lake, MI, USA). A correct hypoxic stimulus was confirmed by measuring hematocrit (Figure 4K and S5C). Age-matched control mice and rats were similarly housed in ambient air outside the chamber. *GFAP-cre/floxed LacZ* or YFP mice used for cell fate mapping were always exposed twice to hypoxia. The first exposure was 7 days long and allowed the activation of the hGFAP-cre construct during the subsequent re-normoxia (14 days long; see Pardal et al., 2007 and Figure S1). For *in vivo* experiments with Tyrphostin AG490, *GFAP-cre/floxed LacZ* mice were injected with AG490 one day before the beginning of the hypoxic period and then three times per week during the exposition to the hypoxic environment (266,7 µg/mouse). Tyrphostin AG490 (5mg; Calbiochem, Millipore) was dissolved in 1 mL of sterile DMSO and brought to a final concentration of 2.2 mM by diluting in sterile PBS 1X. Control mice were injected with equal volume of the vehicle. Each group included the analysis of 3 cell suspensions, each obtained from 2 mice (4 CBs). Animals were maintained in the hypoxic environment for 7 days. For *in vivo* experiments with dimethylxalylglycine (DMOG, Frontier Scientific), normoxic *GFAP-cre/floxed YFP* mice were injected with DMOG intraperitoneally twice per day at a dose of 80 mg/Kg during 12 days. When preparing a 200 mg/mL stock solution of DMOG, the compound was dissolved in DMSO. Fresh working solution was prepared every day, diluting the stock solution to a final concentration of 20 mg/mL in saline and storing it at 4°C in dark for a maximum of 24 h. Normoxic control mice were injected twice daily with vehicle at the same time. In the hypoxic experimental group, animals were exposed during 12 days to chronic hypoxia. Each group included 6-8 mice in order to obtain 3 CB cell dispersions from 2-3 mice each. Mice were housed in standard rodent cages with 24 h access to pellet food and water.

### **Dissociation of Carotid Body Cells**

Rat and transgenic mouse CBs were dissociated by enzymatic treatment in PBS solution containing 0.6 mg/ml collagenase type II (Sigma), and 0.3 mg/ml trypsin (Sigma), for 20 min at 37°C in a crystal flask at 600 rpm in a Thermomixer Comfort (Eppendorf). After enzymatic treatment, 2 volumes of staining solution were added to quench enzymes. Staining solution contained (for 50 ml): 44 ml L15 medium (GIBCO), 0.5 ml penicillin/streptomycin (GIBCO), 0.5 ml 1 M HEPES buffer (GIBCO), 0.1 g BSA (Sigma), and 5 ml distilled and deionized water. Dissociated CB cells were centrifuged for 5 min at 300 g at 4°C. Afterwards, the cell pellet was resuspended and the cells were plated on an ultralow binding well for neurosphere assays, or used for immunocytochemistry.

### **Transfection of Carotid Body or Neurosphere Cells**

Rat CBs were dissociated by enzymatic treatment following the protocol described above. Dissociated cells were plated on ultralow binding wells and transfected with lipofectamine 2000 following vendor instructions (Invitrogen, Life Technologies). For transfection, 2.5 µg of pGFAP-eGFP plasmid was used. After 36h in culture, transfected cells were resuspended and sorted by flow cytometry.

EPAS1 (HIF-2 $\alpha$ ) siRNA experiments were carried out using predesigned SmartPool siRNA (Dharmacon). Neurospheres were dissociated with sequential incubation at 37°C during 10 minutes in papain (28.1 Units per mg of protein, Worthington) at a final concentration of 35 µL/mL in HBSS, and in 0.6 mg/ml collagenase type II (Sigma) at a final concentration of 66 µL/mL in HBSS. NS cells were cultured onto adherent, using 5 µg/mL fibronectin (Biomedical technologies Inc.) to pre-treat the 24-well plates, and with complete neural crest medium, overnight. Initially, to optimize transfection efficiency, EPAS1 knock-down was analyzed by Real Time quantitative PCR, with cells transfected using 25 nM, 50 nM or 100 nM siRNA, complexed to 2 µL of lipofectamine 2000 reagent, following manufacturer instructions (Invitrogen, Life Technologies). EC differentiation assays were performed transfecting NS cells with 50 nM siRNA. After transfection (12-18h later), cells were exposed to hypoxia (3% O<sub>2</sub>) for 24h if used for RNA extraction, or for 72h if used for EC differentiation functional assay. Control cells were transfected with the same amount of control siRNA smart pool (Dharmacon).

### **Neurosphere Assays**

Dispersed rat CB cells were typically cultured in ultralow binding 6-well plates (Corning Inc., Corning, NY) at a clonal density of 10,000 cells per well, so that individual neurospheres were spatially apart from each other. Culture medium contained D-MEM:F-12 (GIBCO BRL, Grand Island, NY) with 15% FBS

(GIBCO), 1% N2 supplement (GIBCO), 2% B27 supplement (GIBCO), 1% penicillin/streptomycin (GIBCO), 20 ng/ml recombinant human bFGF (R&D Systems, Minneapolis, MN), 20 ng/ml recombinant human IGF-1 (R&D Systems), and 20 ng/ml recombinant human EGF (R&D Systems). All cultures were maintained in O<sub>2</sub> and CO<sub>2</sub>-controlled incubators (Thermo Electron Corp., Waltham, MA) at 21% or 3% O<sub>2</sub> and 37°C. Cell cultures exposed to hypoxia were tested for the expression of typical hypoxia-responsive genes to confirm a correct stimulus (Figure 3C and D).

### **Endothelial Differentiation Assay**

To study the induction of endothelial differentiation in adherent NS cultures we exposed cells to different factors: 7 IU/mL erythropoietin (EPO, Binocrit®), 0.1 µM endothelin-1 (ET-1, Sigma), 25 ng/mL platelet-derived growth factor (PDGF, R&D), 25 ng/mL vascular endothelial growth factor (VEGF, R&D), 100 µM adenosine (ADO, Sigma), 10 µM dopamine (DA, Sigma) and 10 µM met-enkephalin (Met-enk, Sigma), or 3% hypoxia. Factors were added every day to standard culture medium without mitogens. For EPO pathway inhibition, EPO (7IU/ml) was added to low serum concentration medium (5% FBS, GIBCO) without mitogens and supplemented, where necessary, with EPO-neutralizing antibody (1:20) (Santa Cruz) or 50 µM Tyrphostin AG490 (Calbiochem). Inhibition of prolyl-hydroxylases during EC differentiation in hypoxic adherent NS cultures was achieved by adding DMOG (Frontier Scientific) daily, dissolved in DMSO, to a final concentration of 0.1 mM or 1 mM. Controls were performed adding the same volume of vehicle.

### **Immunocytochemistry**

Adherent cultures: Adherent neurosphere colonies were fixed in 4% PFA, pre-blocked for at least 1h at room temperature, and incubated with the primary and secondary antibodies for 1h each, at RT. The blocking solution was the same than for tissues (see above). Details about the antibodies used are given in Table S1. Incubation in 1:100 Rhodamine or Fluorescein- conjugated GSA I in PBS during 1 hour at RT was performed prior to DAPI counter-staining.

Cells in suspension: Dispersed CB cells were collected in conical tube, fixed in 4% PFA (prepared in PBS) for 10 min at RT and washed in PBS by centrifuging at 300g 5 minutes at 4°C. Both primary and secondary antibody immunoreaction or Rhodamine conjugated GSA I staining was carried out in PBS with calcium and magnesium plus 10% FBS 1h at RT. Finally, nuclei were counterstained by DAPI. Cells were pulled down on poly-lysine coated slides (Thermo scientific) by centrifuging at 1000 rpm 5 minutes in Shandon Cytospin 4 (Thermo Electron Corporation). Details about the antibodies used are given in Table S1.

### **Fluorescent immunohistochemistry**

Following normoxic/hypoxic treatments, animals were anaesthetized with ketamine (100 mg/kg) plus xylazine (10 mg/kg), intracardially perfused with 4% PFA (Sigma), and the carotid bifurcations dissected and postfixed in PFA for 2 hr. After overnight cryoprotection in 30% sucrose solution (Sigma), bifurcations were embedded in OCT compound (Sakura Finetek) and frozen in dry ice. Sections (10 µm thick) of the carotid body within the carotid bifurcation were cut on a Leica cryostat. For immunohistochemistry we used the standard staining procedure previously published (Pardal et al., 2007). Antibodies used are listed in Table S1. Fluorescent specimens were viewed under a confocal microscope with a 63x immersion-oil objective. Image J software (National Institute of Health, USA) was used for cell number quantifications. In the case of anti-β-Gal antibody, we were only able to analyze 2 normoxic and 2 hypoxic animals due to this antibody running out of production.

For detection of endothelial cells in histological studies we used Griffonia simplicifolia lectin I (GSA I; Vector Labs) (Laitinen, 1987; Bankston et al., 1991). After antibody immunostainings, sections were incubated in GSA I lectin, diluted 1:100 in PBS, for 1h at room temperature. Finally, slides were counter stained with 2.5 mg/ml DAPI (Sigma) for 15 min at room temperature, and then mounted using Fluorogel mounting medium (Electron Microscopy Sciences).

### **DAB immunohistochemistry**

Endogenous peroxidases were inhibited by incubating tissue sections in 0.3% H<sub>2</sub>O<sub>2</sub> and 10% Methanol in PBS, pH 7.4, for 20 minutes at RT. Non-specific antibody binding sites were blocked by incubating in 10% Normal Horse Serum (NHS, GIBCO), 0.3% Triton X-100 in 0.1 M PBS, pH 7.4, for 2 hours at RT. Slices were successively incubated overnight at 4°C with specific anti-GFP primary antibody (see Table S1) diluted in 1% NHS, 0.3% Triton X-100, followed by an incubation with biotinylated Goat anti-rabbit IgG secondary antibody (Vector Labs), diluted 1:1000 in the same diluent used for primary antibody, for 1 hour. Sections were incubated in avidin-biotin-peroxidase complex, diluted 1:100 (ABC kit, Vectastain Elite, Vector Labs), for 30 minutes at RT. Antibody binding sites were revealed incubating sections in



3,3'-diaminobenzidine (DAB; Peroxidase (HRP) Kit, Vector Labs) for 1 minute. Negative controls were obtained by omitting primary antibody. Sections were counterstained with hematoxylin and coverslipped using Eukitt mounting medium (Electron Microscopy Sciences, EMS), after dehydration in a series of ethyl alcohols and xylene.

### **Electron microscopy**

Following normoxic/hypoxic treatments, animals were anaesthetized with ketamine (100 mg/kg) plus xylazine (10 mg/kg) and intracardially perfused with PBS-based 4% PFA (Sigma). Carotid bifurcations were dissected and postfixed in the same fixative for 2 hours. **Bluo-gal staining:** *GFAP-Cre/floxed LacZ* and *Wnt1-Cre/floxed LacZ* CB 50  $\mu$ m thick sections were fixed in 4% PFA in PBS pH 7.4, rinsed twice in PBS, and stained in 2 mM 5-bromo-3-indolyl- $\beta$ -D-galactoside (bluo-gal; Invitrogen Life Technologies) in PBS. Bluo-gal was dissolved in PBS containing 20 mM potassium ferrocyanide, 20 mM potassium ferricyanide, 2 mM MgCl<sub>2</sub> and 0.3% Triton-X, as previously described (Weis et al., 1991; Joseph et al., 2004). The staining was performed for 24 hours at 37°C. Sections were removed from the bluo-gal buffer, rinsed in PBS, then postfixed in 2.5% glutaraldehyde overnight at 4°C in agitation. CB sections were then rinsed in 0.1 M PB pH 7.4 and postfixed in aqueous 1% OsO<sub>4</sub> for 1h at RT. Sections were rinsed in PB then dehydrated in an ethanol series (30, 50, 70, 80, 95 and 100% ethanol) before infiltrating and embedding in Spurr resin (Bozzola and Russell, 1992). Semithin sections (1  $\mu$ m thick) were cut with a glass knife. Ultrathin sections (60 nm) were cut with a diamond knife and examined without further staining to facilitate visualization of the bluo-gal precipitates. Note that the presence of Triton-X detergent in the bluo-gal buffer resulted in poor preservation of membranes. However, Triton-X was required for effective bluo-gal staining.

### **Image acquisition and processing**

**Immunofluorescent images:** Microscope: Olympus BX61; Type/ magnification/ numerical aperture of objectives: UPlanFl/20x/0.50, UPlanFl/40x/0.75, UPlanFl/100x/1.30 with oil immersion; Temperature: RT; Imaging medium: Fluoro-Gel (Electron Microscopy Science); Fluorochromes: Alexafluor 568, Alexafluor 488; Camera: Olympys DP70; Acquisition software: DP Controller; Post-acquisition processing: Photoshop (contrast control by 'Level' tool).

**Bright field images:** Microscope: Olympus BX 61; Type/ magnification/ numerical aperture of objectives: UPlanFl/20x/0.50, UPlanFl/40x/0.75; Temperature: RT; Imaging medium: Eukitt (Electron Microscopy Sciences); Camera: Olympus DP70; Acquisition software: DP Controller; Post-acquisition processing: Photoshop: (brightness/contrast adjustment).

#### **Confocal images:**

- Microscope: Zeiss LSM 7 DUO; Type/ magnification/ numerical aperture of objectives: Plan Aplanachromat/63x/1.40 with oil; Acquisition software: Zeiss Zen2011; Post-acquisition processing: Zeiss Zen2011 Lite (maximum projection and orthogonal view).
- Microscope: Nikon Nikon Eclipse Ti-E; Type/ magnification/ numerical aperture of objectives: Plan Apo/60x/1.40 with oil; Acquisition software: Nikon NIS-Elements C; Post-acquisition processing: Nikon NIS-Elements C (maximum projection and orthogonal view).

All the acquisitions were carried out at room temperature. Imaging medium: Fluoro-Gel (Electron Microscopy Sciences).

**Electron microscopy images:** Microscope: Philips CM-10; Temperature: RT; Acquisition software: iTEM solution SIS (Olympus); Camera: Veleta (Olympus); Post-acquisition processing: Photoshop (brightness/contrast adjustment).

### **Flow Cytometry**

After incubation at 37°C, in ultralow binding wells over night for the antigen retrieval, cells obtained from enzymatic digestion of mouse CBs were resuspended in a volume of 100  $\mu$ L and were incubated for 1 hour in the dark at 4 °C with PE-conjugated monoclonal antibodies against mouse CD31 (BD Biosciences, 1:100). For separating and analyzing GSA I+ cells from the different samples (CBs, NS, or adherent NS), we used a protocol modified from (Sahagun et al., 1989). In the case of flat NS colonies, obtained by culturing NS on fibronectin and in the presence of EPO during 5 days, cells were removed from the petri dish by treating with 0.25% trypsin + 0.1% EDTA for 5 minutes at 37°C. Both CB and NS dissociated cells were re-seeded in ultralow binding wells and incubated at 37°C in complete medium without mitogens overnight. Cells were then pelleted and resuspended in PBS with Calcium and Magnesium supplemented with 10% FCS. FITC-GSA I was added to a final dilution of 1:100, and cells were incubated on ice for 30 minutes. As controls, some tubes received either no lectin or lectin preincubated with 0.2M galactose. After washing off unbound molecules, cells were resuspended in

staining medium containing 2 mg/ml 7-AAD (Molecular Probes). Dead cells were eliminated from sorts and analyses as 7-AAD+.

### **Reverse Transcriptase-Polymerase Chain Reaction and Real Time quantitative PCR**

Total RNA was extracted from GSA I positive and negative cell fractions, sorted from dispersed adherent NS or dispersed rat CBs, using a commercial kit (RNeasy MICRO kit; Qiagen), following manufacturer instructions. In the case of NS, cells were separated after induced endothelial differentiation during 5 days by EPO treatment (see above). For the RNA extraction,  $8-10 \times 10^4$  cells were used. Rat brain, liver, kidney and PC12 cell line were used as positive expression controls and were processed for total RNA extraction using Trizol reagent (Invitrogen), following the protocol recommended by the manufacturer. For retrotranscription, cDNA was synthesized with QuantiTec Reverse transcription kit (Qiagen), as indicated by manufacturer instructions. Standard PCR was performed with 20 ng of first strand cDNA. Loading control used was cyclophilin (CPH). Real-time quantitative PCR was performed in an ABI Prism 7500 Sequence Detection System using the thermocycler conditions recommended by the manufacturer (Applied-Biosystems). Detection was performed with SYBR Green PCR Master Mix.

### **Western blot**

Preparation of cell protein extracts: HUVECs ( $10^6$  cells) were exposed for 3 days to a hypoxic environment (3% O<sub>2</sub>). For preparing whole cell protein extracts, cells were washed once with ice-cold PBS (GIBCO) and lysed with 500  $\mu$ L of lysis buffer (150 mM NaCl, 10 mM Tris pH 7.9, 1 mM EDTA, 1% SDS, 1% Triton X-100 and 1X protease inhibitor cocktail (Roche)) for 20 minutes on ice. The lysates were centrifuged at 15000 X g for 30 minutes at 4°C and supernatants containing proteins were collected and stored at -20 °C. Protein concentration of supernatants were quantified using a protein Bradford assay reagent (Sigma). Aliquots of the supernatants were mixed with 4X reducing loading buffer, boiled for 3 minutes and stored at -20°C until use.

Electrophoresis and immunoblotting: 80  $\mu$ g of total cell lysate per lane was subjected to 12% SDS-PAGE and transferred onto PVDF membrane (0.45 pore size; Millipore). The efficiency of loading transfer was confirmed by staining the PVDF membrane with Ponceau S (Sigma-Aldrich). Filters were blocked 2 hours at RT with 5% nonfat dry milk powder in TBS-T (10 mM Tris pH 7.5, 100 mM NaCl, and 0.05% Tween 20). Membranes were washed in TBS-T and incubated with a Goat polyclonal anti EPO antibody (Santa Cruz) over night at 4°C with gentle shaking.  $\alpha$ -Tubulin (Sigma-Aldrich) served as loading and transfer control. After washing with TBS-T, HRP- conjugated anti-Goat IgG antibody (Biomedal) was added. Immunoreactive proteins were revealed using an enhanced chemiluminescence (ECL) kit (GE Healthcare).

### **Statistics**

Sample size was chosen based on previous results or pilot studies. In any case, we expected to obtain a moderate-to-large effect size to ensure a power of 0.8, and an alpha of 0.05. Additionally, we took into account technical difficulties that could affect the good quality of the samples. Hence, we opted to increase the sample size up to 20% of the initial sample size estimation. In all cases we tried to respect the principles of 3Rs (Replacement, Reduction and Refinement). The experiments were pseudo-randomized with regards to sex (in order to guarantee a 50% of males and females in the different animal groups) and completely randomized with regards to allocation to different experimental groups. The investigator was completely blinded when assessing the outcome. Data are always presented as the mean  $\pm$  standard error of the mean (s.e.m.), and the number of experiments carried out with independent cultures/animals (n) is shown in figure legends.

## Supplemental References

- Arsenault, P.R., Pei, F., Lee, R., Kerestes, H., Percy, M.J., Keith, B., Simon, M.C., Lappin, T.R., Khurana, T.S., and Lee, F.S. (2013). A knock-in mouse model of human PHD2 gene-associated erythrocytosis establishes a haploinsufficiency mechanism. *The Journal of biological chemistry* 288, 33571-33584.
- Bankston, P.W., Porter, G.A., Milici, A.J., and Palade, G.E. (1991). Differential and specific labeling of epithelial and vascular endothelial cells of the rat lung by *Lycopersicon esculentum* and *Griffonia simplicifolia* I lectins. *European journal of cell biology* 54, 187-195.
- Barriga, E.H., Maxwell, P.H., Reyes, A.E., and Mayor, R. (2013). The hypoxia factor Hif-1alpha controls neural crest chemotaxis and epithelial to mesenchymal transition. *The Journal of cell biology* 201, 759-776.
- Benelli, R., and Albin, A. (1999). In vitro models of angiogenesis: the use of Matrigel. *The International journal of biological markers* 14, 243-246.
- Bishop, T., Talbot, N.P., Turner, P.J., Nicholls, L.G., Pascual, A., Hodson, E.J., Douglas, G., Fielding, J.W., Smith, T.G., Demetriades, M., *et al.* (2013). Carotid body hyperplasia and enhanced ventilatory responses to hypoxia in mice with heterozygous deficiency of PHD2. *The Journal of physiology* 591, 3565-3577.
- Bozzola, J.J., and Russell, L.D. (1992). *Electron microscopy: principles and techniques for biologists* (Boston, MA, Jones & Bartlett Publishers).
- Hodson, E.J., Nicholls, L.G., Turner, P.J., Llyr, R., Fielding, J.W., Douglas, G., Ratnayaka, I., Robbins, P.A., Pugh, C.W., Buckler, K.J., *et al.* (2016). Regulation of ventilatory sensitivity and carotid body proliferation in hypoxia by the PHD2/HIF-2 pathway. *J Physiol* 594, 1179-1195.
- Joseph, N.M., Mukoyama, Y.S., Mosher, J.T., Jaegle, M., Crone, S.A., Dormand, E.L., Lee, K.F., Meijer, D., Anderson, D.J., and Morrison, S.J. (2004). Neural crest stem cells undergo multilineage differentiation in developing peripheral nerves to generate endoneurial fibroblasts in addition to Schwann cells. *Development* 131, 5599-5612.
- Kaelin, W.G., Jr., and Ratcliffe, P.J. (2008). Oxygen sensing by metazoans: the central role of the HIF hydroxylase pathway. *Molecular cell* 30, 393-402.
- Kugelmeier, P., Nett, P.C., Zullig, R., Lehmann, R., Weber, M., and Moritz, W. (2008). Expression and hypoxic regulation of the endothelin system in endocrine cells of human and rat pancreatic islets. *JOP : Journal of the pancreas* 9, 133-149.
- Laitinen, L. (1987). *Griffonia simplicifolia* lectins bind specifically to endothelial cells and some epithelial cells in mouse tissues. *The Histochemical journal* 19, 225-234.
- Melero-Martin, J.M., Khan, Z.A., Picard, A., Wu, X., Paruchuri, S., and Bischoff, J. (2007). In vivo vasculogenic potential of human blood-derived endothelial progenitor cells. *Blood* 109, 4761-4768.
- Pardal, R., Ortega-Saenz, P., Duran, R., and Lopez-Barneo, J. (2007). Glia-like Stem Cells Sustain Physiologic Neurogenesis in the Adult Mammalian Carotid Body. *Cell* 131, 364-377.
- Platero-Luengo, A., Gonzalez-Granero, S., Duran, R., Diaz-Castro, B., Piruat, J.I., Garcia-Verdugo, J.M., Pardal, R., and Lopez-Barneo, J. (2014). An o2-sensitive glomus cell-stem cell synapse induces carotid body growth in chronic hypoxia. *Cell* 156, 291-303.

Sahagun, G., Moore, S.A., Fabry, Z., Schelper, R.L., and Hart, M.N. (1989). Purification of murine endothelial cell cultures by flow cytometry using fluorescein-labeled griffonia simplicifolia agglutinin. *The American journal of pathology* *134*, 1227-1232.

Weis, J., Fine, S.M., David, C., Savarirayan, S., and Sanes, J.R. (1991). Integration site-dependent expression of a transgene reveals specialized features of cells associated with neuromuscular junctions. *The Journal of cell biology* *113*, 1385-1397.